This is a repository copy of *The effect of natural organic matter on the adsorption of mercury to bacterial cells*.

White Rose Research Online URL for this paper:
http://eprints.whiterose.ac.uk/127218/

Version: Accepted Version

1 The effect of natural organic matter on the adsorption of mercury to bacterial cells

3 Sarrah Dunham-Cheatham[1‡], Bhoopesh Mishra[2], Satish Myneni[3], and Jeremy B. Fein[1]

5 [1] *Department of Civil and Environmental Engineering and Earth Sciences, University of Notre*
6 *Dame, Notre Dame, IN 46556, USA*
7 [2] *Department of Physics, Illinois Institute of Technology, Chicago, Illinois 60616, USA*
8 [3] *Department of Geosciences, Princeton University, Princeton, NJ 08544, USA*

11 **<u>Abstract</u>**

13 We investigated the ability of non-metabolizing *Bacillus subtilis*, *Shewanella oneidensis*

14 MR-1, and *Geobacter sulfurreducens* bacterial species to adsorb mercury in the absence and

15 presence of Suwanee River fulvic acid (FA). Bulk adsorption and X-ray absorption spectroscopy

16 (XAS) experiments were conducted at three pH conditions, and the results indicate that the

17 presence of FA decreases the extent of Hg adsorption to biomass under all of the pH conditions

18 studied. Hg XAS results show that the presence of FA does not alter the binding environment of

19 Hg adsorbed onto the biomass, regardless of pH or FA concentration, indicating that ternary

20 bacteria-Hg-FA complexes do not form to an appreciable extent under the experimental conditions,

21 and that Hg binding on the bacteria is dominated by sulfhydryl binding. We use the experimental

22 results to calculate apparent binding constants for Hg onto both the bacteria and the FA. The

23 calculations yield similar binding constants for Hg onto each of the bacterial species studied. The

24 calculations also indicate similar binding constants for Hg-bacteria and Hg-FA complexes, and the

25 values of these binding constants suggest a high degree of covalent bonding in each type of

26 complex, likely due to the presence of significant concentrations of sulfhydryl functional groups

27 on each. S XAS confirms the presence of sulfhydryl sites on both the FA and bacterial cells, and

28 demonstrates the presence of a wide range of S moieties on the FA in contrast to the bacterial

29 biomass, whose S sites are dominated by thiols. Our results suggest that although FA can compete

‡ Corresponding author: dr.smdcheatham@gmail.com

30   with bacterial binding sites for aqueous Hg, because of the relatively similar binding constants for

31   the types of sorbents, the competition is not dominated by either bacteria or FA unless the

32   concentration of one type of site greatly exceeds that of the other.

33

34   **<u>Introduction</u>**

35   Heavy metals, such as Hg, adsorb to proton-active functional groups on bacterial cell

36   envelopes (e.g., Beveridge and Murray, 1976; Fortin and Beveridge, 1997; Daughney et al., 2002;

37   Fein, 2006; Kenney and Fein, 2011), affecting the speciation and distribution of these metals in

38   geologic systems. Recent studies (e.g., Guiné et al., 2006; Mishra et al. 2007; 2009; 2010; 2011;

39   Pokrovsky et al., 2012; Song et al., 2012; Colombo et al., 2013) have shown that at least some

40   bacterial cell envelopes contain proton-active sulfhydryl functional groups. Because Hg binds

41   readily and strongly to sulfur compounds (Compeau and Bartha, 1987; Winfrey and Rudd, 1990;

42   Benoit et al., 1999), bacterial adsorption of Hg may dramatically affect the distribution, transport

43   and fate of Hg in geologic systems.

44   Natural organic matter (NOM) is present in nearly every near-surface geologic system, and

45   complexation reactions between metals and NOM can dramatically change the behavior of the

46   metals in the environment (McDowell, 2003; Ravichandran, 2004). NOM molecules contain a

47   range of functional group types, including carboxyl, phenol, amino, and sulfhydryl groups, that

48   have the potential to create highly stable complexes with metal ions across the pH range (Ephraim,

49   1992; Ravichandran et al., 1999; Drexel et al., 2002; Haitzer et al., 2002; Croué et al., 2003;

50   Ravichandran, 2004). Hg binds strongly to the sulfhydryl groups present within the NOM structure

51   (Dong et al., 2011; Muresan et al., 2011). The relative thermodynamic stabilities of Hg-NOM and

52   Hg-bacteria complexes are not well known. Depending on these relative stabilities, the formation

of metal-NOM complexes may decrease adsorption of Hg to bacteria cell envelopes due to a competitive ligand effect, or under certain conditions may increase adsorption of Hg to bacteria due to ternary complexation with NOM. For example, investigating Pb, Cu, and Ni separately, Borrok et al. (2007) found that ternary metal-FA-bacteria complexes form, and that the importance of the complexes is strongly affected by pH. Conversely, Wightman and Fein (2001) found that the presence of NOM decreases the amount of Cd adsorbed to bacteria under mid- and high-pH conditions, and that the presence of Cd does not affect the adsorption of NOM to bacteria, suggesting that ternary complexes do not occur. No studies have been conducted to date to determine the effects of NOM on Hg binding to bacteria. However, because Hg forms strong complexes both with cell envelopes (Daughney et al., 2002; Mishra et al., 2011; Dunham-Cheatham et al.) and NOM (Loux et al., 1998; Ravichandran, 2004; Skyllberg et al., 2006), it is likely that significant changes to Hg adsorption behavior occur in the presence of NOM.

In this study, we use bulk adsorption and Hg X-ray absorption spectroscopy (XAS) experiments, conducted as a function of pH and FA concentration, using intact non-metabolizing bacterial cells to study Hg binding onto three different bacterial species and to compare the ability of bacteria to adsorb mercury in the presence and absence of a fulvic acid (FA). We use the experimental results to calculate apparent stability constants for Hg-bacteria and Hg-FA complexes, allowing for quantitative modeling of the competitive binding that can occur between bacteria and FA in more complex settings. This study examined both Gram-positive and Gram-negative bacterial species in order to determine if cell envelope structure affects the binding reactions, and one species was a Hg methylator, which we examined in order to determine if the extent or nature of Hg binding onto that species differed from that exhibited by the non-methylators.

Methods

78 **Experimental methods**

79 *Bacterial growth and washing procedure*

80   *Bacillus subtilis* (a Gram-positive aerobic soil species) and *Shewanella oneidensis* MR-1

81 (a Gram-negative facultative anaerobic species) cells were cultured and prepared following the

82 procedures outlined in Borrok et al. (2007). Briefly, cells were maintained on agar plates consisting

83 of trypticase soy agar with 0.5% yeast extract added. Cells for all experiments were grown by first

84 inoculating a test-tube containing 3 mL of trypticase soy broth with 0.5% yeast extract, and

85 incubating it for 24 h at 32 °C. The 3 ml bacterial suspension was then transferred to 1 L of

86 trypticase soy broth with 0.5% yeast extract for another 24 h on an incubator shaker table at 32 °C.

87 Cells were pelleted by centrifugation at 8100 g for 5 min, and rinsed 5 times with 0.1 M $NaClO_4$.

88   *Geobacter sulfurreducens* (a Gram-negative species capable of Hg methylation) cells were

89 cultured and prepared using a different procedure than detailed above. Cells were maintained in

90 50 mL of anaerobic freshwater basal media (ATCC 51573) at 32 °C (Lovely and Phillips, 1988).

91 Cells for all experiments were grown by first inoculating an anaerobic serum bottle containing 50

92 mL of freshwater basal media, and incubating it for 5 days at 32 °C. Cells were pelleted by

93 centrifugation at 8100 g for 5 minutes, and rinsed 5 times with 0.1 M $NaClO_4$ stripped of dissolved

94 oxygen by bubbling a 85%/5%/10% $N_2/H_2/CO_2$ gas mixture through it for 30 minutes. After

95 washing, each of the three types of bacteria was then pelleted by centrifugation at 8100 g for 60

96 minutes to remove excess water in order to determine the wet mass so that suspensions of known

97 bacterial concentration could be created. All bacterial concentrations in this study are given in

98   terms of gm wet biomass per liter. Bacterial cells were harvested during stationary phase, and all

99   experiments were performed under non-metabolizing, electron donor-free conditions.

100

101   *Adsorption experiments*

102   To prepare experiments, aqueous Hg, NOM, and suspended bacteria stock solutions were

103   mixed in different proportions to achieve the desired final concentrations for each experiment. The

104   experiments were conducted in sets with constant pH (at pH 4.0 ± 0.1, 6.0 ± 0.1, or 8.0 ± 0.3) and

105   constant bacterial concentration (0.2 g bacteria L^{-1} in all cases) at three different FA concentrations

106   (0, 25, or 50 mg L^{-1}), with Hg log molalities ranging from -6.30 to -5.00 (0.1 to 2.0 mg L^{-1}).

107   FA stock solutions were prepared in Teflon bottles by dissolving dried, powdered

108   International Humic Substances Society Suwannee River FA Standard I in a 0.1 M $NaClO_4$ buffer

109   solution to achieve the desired final FA concentration for each experiment. A known mass of wet

110   biomass was then suspended in the FA stock solution, and the pH of the FA-bacteria parent

111   solution was immediately adjusted to the experimental pH using 0.2 M HNO_3 and/or NaOH. To

112   prepare experimental solutions, aliquots of the FA-bacteria parent solution were added

113   gravimetrically to Teflon reaction vessels, followed by a small aliquot of commercially-supplied

114   1,000 mg L^{-1} Hg aqueous standard to achieve the desired final Hg concentration. The pH of each

115   suspension was again adjusted immediately to the experimental pH. The vessels were placed on

116   an end-over-end rotator to agitate the suspensions for the duration of the experiment (2 h for *B.*

117   *subtilis* and *G. sulfurreducens* and 3 h for *S. oneidensis* MR-1, as determined by initial kinetics

118   experiments (results not shown)). The pH of the suspensions was monitored and adjusted every 15

119   minutes throughout the duration of the experiment, except during the last 30 minutes, when the

120   suspensions were undisturbed. At the completion of each experiment, the pH of the suspensions

121   was measured and the experimental suspensions were centrifuged at 8100 g for 5 minutes. The

122   aqueous phase was collected for Hg analysis by inductively-coupled plasma optical emission

123   spectroscopy (ICP-OES), and the solid phase of some of the runs was collected for XAS analyses.

124   Duplicate experiments were performed for each experimental condition.

125

126   *ICP-OES measurements*

127   ICP-OES standards were prepared gravimetrically by diluting a commercially-supplied

128   1,000 mg L^{-1} Hg aqueous standard with pH-adjusted 0, 25, or 50 mg L^{-1} FA stock solution made

129   in 0.1 M $NaClO_4$ so that the pH, ionic strength, and FA concentration of the standards closely

130   matched that of the samples. We found significant interference when standards and samples were

131   not closely matched in this way. The log molality of the Hg standards ranged from -6.60 to -5.00.

132   The standards and samples were all stored in Teflon containers and analyzed with a Perkin Elmer

133   2000DV ICP-OES at wavelength 253.652 nm within 1 day of collection. The set of standards was

134   analyzed before and after all of the samples were analyzed, as well as after every 15 samples, to

135   check for machine drift. Analytical uncertainty, as determined by repeat analyses of the standards,

136   was ± 2.8% for the 0 mg L^{-1} FA samples, ± 7.7% for the 25 mg L^{-1} FA samples, and ± 9.5% for

137   the 50 mg L^{-1} FA samples. Neither standards nor samples were acidified prior to analysis. FA

138   concentration strongly affected system performance and signal strength, likely due to spectral

139   interferences caused by the FA molecule. For each pH and FA concentration condition studied, we

140   conducted biomass-free control experiments to determine the extent of Hg loss due to adsorption

141   onto the experimental apparatus as well as any interferences caused by the presence of FA during

142   the ICP-OES analysis.

143

XAS measurements

145   Hg L_{III}-edge X-ray absorption near edge structure (XANES) and extended X-ray

146   absorption fine-structure spectroscopy (EXAFS) measurements were performed at the MRCAT

147   sector 10-ID beamline (Segre et al., 2000), Advanced Photon Source, at Argonne National

148   Laboratory. The continuous-scanning mode of the undulator was used with a step size of 0.5 eV

149   and an integration time of 0.1 sec per point to decrease the radiation exposure during a single scan.

150   Additionally, measurements were made at different spots on the samples to further decrease the

151   exposure time. Hg XAS measurements were collected as described in Mishra et al. (2011).

152   Crystalline powder standards (cinnabar [red HgS] and mercuric acetate) were measured

153   and used to calibrate the theoretical calculations against experimental data. Data from the standards

154   were analyzed to obtain the S02 parameter, where S02 is the value of the passive electron reduction

155   factor used to account for many-body effects in EXAFS. By fixing the values of S and O atoms to

156   2 in cinnabar and mercuric acetate, we obtained $S0^2$ values of 1.02 ± 0.05 and 0.98 ± 0.03,

157   respectively. Hence, we chose to set the value of $S0^2 = 1.0$ for all samples. Fitting of the powder

158   standards to their known crystallographic structures (cinnabar and mercuric acetate) reproduced

159   the spectral features in the entire fitting range (1.0–4.2 Å), and fitting parameters were in

160   agreement with previously reported values. Only the paths necessary to model the solid standards

161   were used for fitting the solution standards and the unknown Hg samples.

162   Two Hg species, Hg-cysteine and Hg-acetate, were utilized as solution-phase standards for

163   Hg XAS analyses. First, an aqueous Hg^{2+} standard was prepared from high-purity 5 mM Hg^{2+} in

164   5% HNO_3 and was then adjusted to pH 2.0 ± 0.1 for measurement by adding appropriate amounts

165   of 5 M NaOH. A Hg-cysteine standard was prepared by adding cysteine to the aqueous Hg^{2+}

166   standard to achieve a Hg:ligand ratio of 1:100. The pH of the Hg-cysteine standard was adjusted

167   to 5.0 ± 0.1 by adding appropriate amounts of 1 M or 5 M NaOH. A Hg-acetate standard was

168   prepared by adding mercuric acetate salt to milliQ water and adjusting the pH to 5.0 ± 0.1 by

169   adding appropriate amounts of 1 M or 5 M NaOH.

170   Sulfur K-edge XANES spectra for biomass and FA samples were acquired at sector 9-BM

171   of the Advanced Photon Source at Argonne National Laboratory using Lytle detector in

172   fluorescence detection mode. At 9-BM, signal from higher order harmonics was removed by

173   detuning the monochromator to 70% of maximum beam flux at 2472.0 eV. Energy calibration was

174   performed by setting the first peak in the spectrum of sodium thiosulfate salt ($Na_2S_2O_3$) to 2469.2

175   eV. XANES spectra were measured between 2450 and 2500 eV. Step sizes in the near-edge region

176   (2467-2482 eV) were 0.08 eV, and 0.2 eV in pre- and post- edge regions, respectively. Samples

177   were smeared on carbon tape and the data were collected under a He atmosphere.

178   For this study, sulfur species are divided into three main categories and referred to as

179   reduced S (below 2472 eV), sulfoxide S (near 2473.5 eV), and oxidized S (above 2476.5 eV).

180   Accordingly, three commercially-supplied (Sigma Aldrich) S standards, cysteine, dimethyl

181   sulfoxide (DMSO), and sodium dodecyl sulfate (NaDS), were used to fingerprint S speciation. S

182   standards were mixed with a dry powder of polyacrylic acid (PAA) to achieve a mixture containing

183   ~1% total S by mass. To perform S XANES measurements, a thin layer of a PAA-S standard

184   mixture was smeared on a carbon tape. All standards were prepared within 12 hours of analysis.

185   To prepare Hg XAS samples, FA was reacted with Hg by diluting a commercially-supplied

186   1000 mg L^{-1} Hg standard with a pH-adjusted 50 mg L^{-1} FA stock solution prepared in 0.1 M

187    $NaClO_4$. The log molalities of Hg investigated were -4.30 and -3.60 at both pH 4.00 ± 0.10 and

188   8.00 ± 0.10 for each Hg concentration. *S. oneidensis* MR-1 biomass was also reacted with Hg in

189   the presence and absence of FA to ascertain possible effects of FA on the Hg binding environment

190   on the bacterial cell envelopes. Biomass was collected from the experiments with -5.30 log M Hg,

191   pH values 4.00 ± 0.10 or 8.00 ± 0.10, and 50 mg L^{-1} FA. Samples were loaded into slotted Plexiglas

192   holders that were subsequently covered with Kapton tape with a Kapton film sandwiched in

193   between the tape and plexiglass to avoid direct contact of the sample with the tape adhesive.

194   Samples were refrigerated until data collection. All measurements were conducted within 48 hours

195   of sample preparation.

196   The data were analyzed by using the methods described in the UWXAFS package (Stern

197   et al., 1995). Energy calibration between different scans was maintained by measuring Hg/Sn

198   amalgam on the reference chamber concurrently with the fluorescence measurements of the

199   biomass-bound Hg samples (Harris et al., 2003). The inflection point of the Hg L$_{III}$-edge (12.284

200   KeV) was used for calibration. Data processing and fitting were done with the ATHENA and

201   ARTEMIS programs (Ravel and Newville, 2005). The data range used for Fourier transformation

202   of the k-space data was 2.0–9.5 Å^{-1}. The Hanning window function was used with dk = 1.0 Å^{-1}.

203   Fitting of each spectrum was performed in r-space, at 1.2-3.2 Å, with multiple k-weighting (k^1, k^2,

204   k^3) unless otherwise stated. Lower χ_v^2 (reduced chi square) was used as the criterion for inclusion

205   of an additional shell in the shell-by-shell EXAFS fitting procedure.

206

207   **Thermodynamic modeling**

208   Surface-complexation models were constructed to model Hg binding with bacterial cell

209   envelope functional groups and with those on the FA molecules, and to quantify the competition

210   between the two. Observed adsorption reactions between aqueous Hg species and deprotonated

211   bacterial cell envelope sites and/or FA binding sites were modeled according to the following

212   generic reaction:

9

213    $$Hg\ species^{x+} + R\text{-}A_i^- \Leftrightarrow (R\text{-}A_i)(Hg\ species)^{(x-1)+} \tag{1}$$
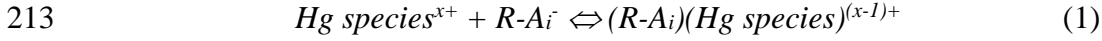
214   where '$Hg\ species^{x+}$' represents the specific aqueous Hg species considered, '$R\text{-}A_i$' represents the

215   deprotonated cell or FA binding site, '$(R\text{-}A_i)(Hg\ species)$' represents the Hg-bacterial cell envelope

216   or Hg-FA complex, and the 'x' represents the charge of the aqueous Hg species. Stability constants

217   for each of the Hg-bacterial cell envelope and Hg-FA complexes are expressed as the

218   corresponding mass action equation for Reaction (1):

219    $$K_{ads} = \frac{[(R - A_i)(Hg\ species)^{(x-1)+}]}{a\,(Hg\ species^{x+})\,[R - A_i^-]} \tag{2}$$

220   where K_{ads} is the thermodynamic equilibrium constant for Reaction (1), the square brackets

221   represent concentrations in mol L^{-1}, and a represents the activity of the species in parentheses.

222   We used FITEQL 2.0 (Westall, 1982) for the equilibrium thermodynamic modeling of the

223   adsorption data, using the aqueous speciation equilibria and equilibrium constants given in Table

224   S1, and using the Davies equation within FITEQL to calculate activity coefficients. Because all of

225   our experiments were conducted at the same ionic strength, we applied a non-electrostatic model

226   to account for the Hg adsorption data. Bacterial site concentrations and acidity constants used in

227   the calculations for *B. subtilis,* for *S. oneidensis* MR-1, and for *G. sulfurreducens* are from Fein et

228   al. (2005), Mishra et al. (2010), and Dunham-Cheatham et al., respectively. The objective of the

229   modeling exercise was not to construct precise site-specific mechanistic binding models, but rather

230   to provide a quantitative means of estimating the competitive binding of bacteria and FA under a

231   range of relative concentration conditions. Toward this end, because specific binding constants for

232   Hg with each site type on the FA molecule are not known, we modeled Hg binding with the FA as

233   a single complexation reaction between Hg^{2+} and the deprotonated form of a generic FA site. We

234   assumed that this generic binding site exhibits an acidity constant equal to the average of the acidity

235   constants of all of the FA sites, with a site concentration equal to the total concentration of all FA

10

236   sites, using the average values from Borrok and Fein (2004) as a model of the FA site speciation.

237   The calculated acidity constant and site concentration for this generic site are listed in Table S1.

238

239   **Results**
240   *Adsorption experiments*

241   Consistent with previous studies of Hg adsorption onto bacteria (Daughney et al., 2002;

242   Dunham-Cheatham et al.), we observed extensive adsorption of Hg onto the bacterial species

243   studied in the absence of FA, with the extent of adsorption relatively independent of pH between

244   pH 4 and 8 (Figure 1, top plots). For example, approximately 77% of the Hg in a 2 mg L^{-1} Hg

245   solution adsorbs at pH 4 onto 0.2 g L^{-1} *S. oneidensis* MR-1, while approximately 75% adsorbs at

246   pH 8. The presence of FA decreases the amount of Hg adsorbing to cell envelopes of each of the

247   bacterial species and at each of the pH conditions studied (Figure 1, middle and bottom plots).

248   With 50 mg L^{-1} FA, the extent of adsorption at pH 4 decreases to 65%, and at pH 8 to 50%. Our

249   experimental results also indicate that the three bacterial species studied here exhibit similar

250   extents of Hg adsorption under each experimental condition, consistent with the observations from

251   a number of previous studies (e.g. Cox et al., 1999; Yee and Fein, 2001; Borrok et al., 2005,

252   Johnson et al., 2007). Our data suggest that as the concentration of FA increases, so does the

253   amount of Hg remaining in solution. These results indicate that FA competes with the bacterial

254   cells for the adsorption of Hg, and that the adsorption of Hg to FA results in a competitive ligand

255   effect. As a result, less Hg is available for adsorption to proton-active functional groups on the

256   bacterial cell envelope, and less Hg is removed from solution. These results are not surprising, as

257   FA molecules contain sulfhydryl groups within their structure and sulfhydryl groups bind strongly

258   with Hg (Xia et al., 1999; Hesterberg et al., 2001; Drexel et al., 2002; Haitzer et al., 2002; 2003),

259   leading to effective competition with bacterial cell envelopes which also contain proton-active

260   sulfhydryl functional groups (Guiné et al., 2006; Mishra et al., 2007; 2009; 2010; 2011; Pokrovsky

261   et al., 2012; Song et al., 2012; Colombo et al., 2013). In our experimental systems, FA binding

262   sites outnumber those present on the bacteria. For example, 50 mg L^{-1} FA corresponds to

263   approximately 2.8 x 10^{-4} moles of sites L^{-1} (Borrok and Fein, 2004), while 0.2 g L^{-1} *B. subtilis*

264   biomass contains 4.7 x 10^{-5} total moles of sites L^{-1}. At pH 8, 50 mg L^{-1} FA does diminish the extent

265   of Hg adsorption, but only from approximately 75% (with no FA present) to 50%. It appears that

266   given equal site concentrations, bacterial binding of Hg would dominate the competition with FA.

267

268   *Hg XANES and EXAFS*

269   To probe the effect of FA on Hg binding mechanisms with bacterial biomass, we

270   examined Hg-biomass binding at pH 4 and 8 in the presence and absence of a stoichiometric

271   excess of FA (1 mg L^{-1} Hg and 50 mg L^{-1} FA) using Hg L_{III} edge XANES and EXAFS. For the

272   XAS studies, *S. oneidensis* MR-1 was chosen to represent the bacterial species used in this study.

273   Figure 2 shows a comparison between Hg XANES for Hg bound : 1) to FA and to *S. oneidensis*

274   MR-1 biomass at pH 4, 2) to *S. oneidensis* MR-1 biomass in the presence and absence of FA at

275   pH 4, 3) to *S. oneidensis* MR-1 biomass in the presence and absence of FA at pH 8, and 4) to

276   cysteine, and to acetate. Hg XANES data indicate that Hg is complexed with thiol groups in the

277   Hg-biomass samples. Spectral features supporting this conclusion are the small pre-edge peak

278   and the slight dip at 12300 eV in the Hg-biomass XANES data similar to that present in the Hg-

279   cysteine data. This finding is consistent with a previous study which showed Hg binding with

280   sulfhydryl groups on *B. subtilis* cell envelopes under similar experimental conditions (Mishra et

281   al., 2011). The Hg-FA XANES data exhibits a small pre-edge peak similar to that present in the

282   Hg-cysteine data, which confirms that Hg is bound predominantly with the high-affinity thiol

12

283 groups in FA under the experimental conditions. The absence of the dip in the Hg-FA XANES at

284 12300 eV, however, indicates differences in the coordination environment of Hg between FA

285 and bacterial biomass. To understand these subtle differences in XANES, a linear combination

286 fitting of the first derivative of Hg-FA XANES data was performed which resulted in about 90%

287 contribution from Hg-cysteine binding and about 10% contribution from Hg-carboxyl binding

288 (figure S2a). The first derivative of Hg-cysteine standard reproduced the Hg-biomass data

289 confirming that the entire budget of Hg complexation with biomass was accounted by

290 complexation of Hg with thiols. XANES spectra of Hg reacted with *S. oneidensis* MR-1 biomass

291 in the presence and absence of FA at pH 4 and 8 are reproducible, confirming that the binding

292 mechanism of Hg with *S. oneidensis* MR-1 biomass does not change appreciably in the presence

293 of FA.

294 Hg EXAFS results are consistent with the Hg XANES results described above. Differences

295 between the coordination environment of Hg-FA and Hg-biomass is more pronounced in the $k^2\chi(k)$

296 EXAFS data (Figure S1). Low signal to noise ratio in the aqueous Hg-FA data does not allow for

297 a meaningful Fourier Transform (FT) of the Hg-FA EXAFS data. EXAFS $k^2\chi(k)$ and FT data

298 between FA-bearing and FA-free Hg-biomass samples are similar (Figure S1), validating the Hg

299 XANES results. Figure S2b shows a comparison between the FT Hg EXAFS data for Hg bound

300 to *S. oneidensis* MR-1 biomass in the presence and absence of FA at both pH 4 and 8 and their

301 corresponding EXAFS fits. EXAFS fitting parameters are shown in Table S2. It is worth pointing

302 out that although Hg-cystein standard showed a bond distance of 2.32 Å, Hg-biomass samples at

303 pH 4 and 8 had a bond distance of 2.35 Å. This should not be considered a discrepancy because

304 Hg-S distances can vary from 2.32 to 2.36 Å for $Hg(SR)_2$ complexes (Manceau,and Nagy 2008).

305 Similarly, Hg-S distances can range from 2.40 to 2.51 Å for $Hg(SR)_3$ complexes, and 2.50–2.61 Å for

306 $Hg(SR)_4$ complexes.

307
308

309   Taken together, Hg XANES and EXAFS results indicate that Hg binds predominantly to

310   the high-affinity thiol groups on bacterial cell envelopes in the presence and absence of FA and

311   Hg binding mechanisms with bacterial biomass do not change in the presence of FA, excluding

312   the possibility of the formation of a ternary complex. Additionally, Hg XAS results show that pH

313   does not affect the adsorption mechanism of Hg onto biomass in the presence of FA, which is

314   consistent with the similar extent of Hg adsorption as a function of pH described above. However,

315   it is important to note that Hg binding mechanisms with bacterial biomass may be affected by FA

316   at high Hg loadings, where Hg is primarily bound to biomass via lower-affinity carboxyl functional

317   groups. Hg XAS results suggest that S functional groups on *S. oneidnensis* MR-1 cell envelopes

318   outcompete S functional groups in FA for Hg binding. In other words, on average Hg binding to

319   FA appears weaker than Hg binding to bacterial biomass. S XANES was conducted to identify the

320   differences in complexation behavior of Hg with S functional groups on FA and bacterial biomass.

321   S K-edge XANES is highly sensitive to changes in the electronic environment of the sulfur

322   absorber (Xia et al., 1998). Although S K-edge XANES spectra were collected on a large number

323   of standards, in this study we have divided S species into three main categories: reduced S (below

324   2472 eV), sulfoxide S (near 2473.5 eV), and oxidized S (above 2476.5 eV). The S XANES spectra

325   for cysteine, dimethyl sulfoxide (DMSO), and sodium dodecyl sulfate (NaDS) are shown in Figure

326   3a. Species with very different S oxidation states, such as cysteine, sulfoxide, and ester sulfate, are

327   easily resolved in the XANES spectrum. However, resolving one species from another within these

328   three energy ranges is challenging. Reduced S species, including thiols, sulfides, polysulfides, and

329   thiophenes, all give white-line features occurring between 2469 and 2472 eV. More extensive

330   model libraries that include XANES spectra of organic and inorganic S compounds are available

331   in the literature (Myneni, 2002; Vairavamurthy, 1998).

332   Speciation of S in *S. oneidensis* MR-1 biomass was easily identified because the peak

333   energy position of S XANES measurement on the biomass overlapped with the cysteine peak

334   position (Figure 3b). Figure 3b shows the dramatic differences between S XANES on *S. oneidensis*

335   MR-1 cells and Suwanee River FA. S XANES comparing FA with *S. oneidensis* MR-1 shows that

336   nearly the entire S budget of the biomass is present as thiol groups, which are known to form strong

337   bonds with Hg. However, FA has a range of reduced S (including reactive thiol) groups and a large

338   fraction of oxidized S species, consistent with previous observations (Morra et al., 1997). Morra

339   et al., 1997 suggest that a significant fraction of sulfur in SR Fulvic acid is found in oxidized (+5

340   oxidation state) form, followed by smaller fractions in reduced forms (-0.3 ±1.0 and 1.7 oxidations

341   states) respectively. Similarly, Einsiedl et al., 2007 used S XANES to estimate that soil FAs

342   contain around 51% oxidized (S_{+4}, S_{+5}, S_{+6}) and 49% reduced (S_{-1}, S_0, S_{+2}) sulfur species. The

343   reduced S species was dominated by thiols, thiophene and disulfide. Such a dramatic difference

344   between the S budget of FA and bacterial biomass could result in diverse reactivities and stabilities

345   of Hg-S complexes between the two. A detailed study of the reactivity and stability of Hg with FA

346   and bacterial biomass is beyond the scope of this study.
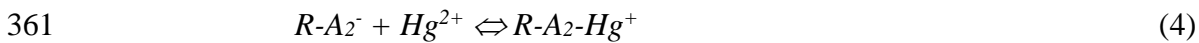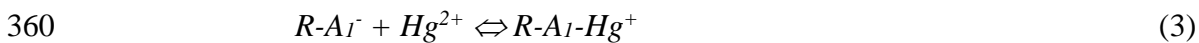
347

348   **Discussion**

349   The experimental results presented here suggest that bacterial cell envelope functional

350   groups and FA functional groups exhibit different binding affinities for Hg under the experimental

351   conditions. Hg binding onto the bacterial cell envelopes is extensive, and although Hg binds

352   strongly with FA, especially with the sulfhydryl groups present within FA (Xia et al., 1999;

353   Hesterberg et al., 2001; Drexel et al., 2002; Haitzer et al., 2002; 2003), the presence of even up to

15

354 50 ppm FA with only 0.2 g (wet mass) L^{-1} of bacteria does not cause the speciation of Hg to be

355 dominated by the FA. The results suggest there is a possibility for competition between the

356 bacterial and FA binding sites for the available Hg.

357   In order to quantify the competitive binding, we use a semi-empirical surface complexation

358 approach. First, we use the FA-free adsorption data at pH 4, 6, and 8 to solve for equilibrium

359 constants for the following Hg^{2+} adsorption reactions, respectively:

360                            $R\text{-}A_1^- + Hg^{2+} \Leftrightarrow R\text{-}A_1\text{-}Hg^+$ (3)

361                            $R\text{-}A_2^- + Hg^{2+} \Leftrightarrow R\text{-}A_2\text{-}Hg^+$ (4)

362                            $R\text{-}A_3^- + Hg^{2+} \Leftrightarrow R\text{-}A_3\text{-}Hg^+$ (5)

363 where $R\text{-}A_1$, $R\text{-}A_2$, and $R\text{-}A_3$ represent the bacterial functional groups with the three lowest pKa

364 values, respectively. At pH 4, the $R\text{-}A_1$ sites are the dominant deprotonated sites available for Hg^{2+}

365 binding for each bacterial species; at pH 6, both $R\text{-}A_1$ and $R\text{-}A_2$ sites are deprotonated; and at pH

366 8, $R\text{-}A_1$, $R\text{-}A_2$, and $R\text{-}A_3$ sites likely contribute to the binding of Hg^{2+}. Therefore, we used the pH 4

367 data to constrain the stability constant value for Reaction (3) alone, then fixed that value and used

368 the pH 6 data to solve for the stability constant value for Reaction (4) with a model that involved

369 Reactions (3) and (4) simultaneously. We then used the values that we calculated for the stability

370 constants for Reactions (3) and (4) and the pH 8 data to solve for the best-fitting value for Reaction

371 (5) with a model that involved Reactions (3) - (5) simultaneously. This modeling approach assumes

372 that Hg^{2+} binding at a given pH occurs dominantly onto sites with pKa values lower than the pH

373 of the experiments; that is, dominantly onto deprotonated sites. However, the resulting stability

374 constant values, which are tabulated in Table 1, yield excellent fits to the FA-free Hg adsorption

375 data as a function of pH and Hg loading (e.g., Figure 4). The calculated stability constants for each

376 reaction for each bacterial species studied here are similar to each other. The log stability constant

16

377   values for Reaction (3) range from 7.3 for *B. subtilis* to 7.8 for *G. sulfurreducens*; those for

378   Reaction (4) range from 11.2 for *S. oneidensis* MR-1to 11.6 for both *B. subtilis* and *G.*

379   *sulfurreducens*; and those for Reaction (5) range from 15.6 for *S. oneidensis* MR-1 to 16.5 for *G.*

380   *sulfurreducens*. The fact that the stability constant values increase by four-to-five orders of

381   magnitude from one site to the next likely is due to the simplified nature of the adsorption model.

382   We assume that Hg^{2+} is the adsorbing aqueous Hg species under all pH conditions. However,

383     $Hg(OH)_2$ is the dominant aqueous Hg species under the experimental conditions, and the

384   concentration of Hg^{2+} is small and becomes smaller with increasing pH over the pH range of our

385   experiments. Therefore, because the extent of adsorption is relatively pH independent, the stability

386   constants that describe adsorption of Hg^{2+} onto bacterial binding sites must become larger with

387   each site considered.

388   Site-specific Hg binding constants have not been determined for Suwanee River FA, so we

389   could not compare the measured effects of the presence of FA with those we would predict from

390   speciation calculations. However, we used the measured extents of Hg adsorption in the presence

391   of FA to calculate empirical generic site Hg binding constants for the FA. That is, we modeled the

392   Hg binding onto the FA with the following single site reaction:

393                   $FA^- + Hg^{2+} \Leftrightarrow FA\text{-}Hg^+$ (6)

394   where FA^- represents the generic deprotonated site on the FA molecule. We modeled this site as a

395   hybrid of the 4 sites used by Borrok and Fein (2004) to account for FA protonation behavior, with

396   the pKa value of the hybrid FA site equal to the average of the pKa values used by Borrok and

397   Fein (2004) and the site concentration equal to the average of the total of the 4 sites for all 9 FAs

398   modeled by Borrok and Fein (2004). Clearly, modeling Hg^{2+} adsorption onto this hybrid generic

399   FA binding site is a simplification of the complex binding environment of Hg on the FA molecule,

400   but it allows us to quantify the competition between the FA and the bacterial cell envelope, and to

401   calculate quantitative estimates of the effects of each binding environment in more complex

402   settings.

403   The calculated stability constants, tabulated in Table 1, yield an excellent fit to the observed

404   effects of the presence of FA on Hg adsorption onto the bacteria studied here (e.g., Figure 4). The

405   stability constants that we calculated for the three bacterial species are similar to each other and

406   do not vary systematically between bacterial species. Additionally, the 25 mg L^{-1} FA data yield

407   calculated Hg-FA stability constant values that are not significantly different from those calculated

408   using the 50 mg L^{-1} FA data. The calculated stability constant values do change systematically

409   with pH, with values increasing with increasing pH. This trend is likely a result of the

410   oversimplification of our Hg-FA binding model; it is probable that the FA molecule contains

411   multiple functional group types that deprotonate sequentially with increasing pH, not just the one

412   site type that we assumed in our models. However, the calculated log stability constant values are

413   not strongly dependent upon pH, with the largest spread being from 13.4 to 14.9 for the pH 4 to 8,

414   25 mg L^{-1} FA data for *B. subtilis*. Thus, the values in Table 1 can be used to yield reasonable

415   estimates of the competition between bacteria and FA in the pH and FA:bacteria concentration

416   ratio conditions studied here.

417   The calculated K values can be used to illustrate the direct competition between bacteria

418   and FA for available aqueous Hg^{2+}. For example, the competition reaction between bacterial site

419   A2 and the FA binding site can be expressed as:

420        $$R\text{-}A_2\text{-}Hg^+ + FA^- \Leftrightarrow FA\text{-}Hg^+ + R\text{-}A_2^- \qquad\qquad (7)$$
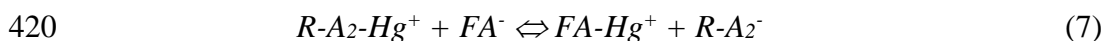
421   where the log equilibrium constant for Reaction (7) can be calculated as the log K value for

422   Reaction (6) minus the log K value for Reaction (4), or values of 2.4 for *B. subtilis*, 3.0 for *S.*

18

423   *oneidensis* MR-1, and 2.6 for *G. sulfurreducens* under pH 6 conditions with 50 mg L^{-1} FA, 0.2 g

424   L^{-1} bacteria. These calculated equilibrium constant values for Reaction (7) can be used to quantify

425   the distribution of Hg between bacterial and FA binding sites for conditions with different relative

426   concentrations of each site type, and the large positive values suggest that on a mass normalized

427   basis, bacterial binding of Hg is greater than that exhibited by FA. Although both bacteria and FA

428   contain sulfhydryl binding sites that are especially effective at binding Hg, our results suggest that

429   these sites may exhibit a higher density on bacteria than they do on FA. It is likely that the FA

430   contains binding sites with a range of Hg binding constants. The binding constants determined by

431   the simplified thermodynamic modeling described above represents an averaging of several site

432   types, some of which have larger binding constants than do the binding sites on the cell envelopes,

433   accompanied by a large number of site with binding constants that are smaller than those on the

434   cell envelopes. The resulting averaged Hg binding constant that we calculate for the FA is similar

435   to those that we calculate for the bacterial biomass. These general conclusions about the S binding

436   mechanisms on the FA and on the bacteria are supported by our S XANES data, which demonstrate

437   that the FA contains a wide range of S moieties while the bacterial biomass is dominated by a

438   single thiol-type S moiety.

439

440   **<u>Conclusions</u>**

441   The results from this study show that the presence of FA decreases the extent of Hg

442   adsorption onto three different bacterial species through competitive binding of the Hg. The

443   presence of the FA does not change the binding environment of Hg on the bacteria, indicating a

444   lack of ternary complexation between the Hg, the FA, and the bacteria. The binding of Hg to both

445   the bacteria and the FA under the experimental conditions is dominated by sulfhydryl binding to

446   both ligands, and the similarities between the binding environments likely results in the

447   competitive balance between them. We use the experimental results to calibrate a quantitative

448   semi-empirical model of the binding of Hg to bacteria and FA, and the stability constants that we

449   calculate can be used to estimate the distribution and speciation of Hg in bacteria- and FA-bearing

450   geologic systems. Because accessibility of Hg to bacteria for metabolic processes such as

451   methylation may be controlled by adsorption, the stability constants calculated in this study may

452   also be useful in estimating the bioavailability of Hg in soil and groundwater systems that contain

453   significant concentrations of FA.

454

Tables

464 Table 1: Calculated log stability constant values for Reactions (3) - (6).

465

[FA] (mg L^{-1})	pH	Bacteria	Reaction (3)[a]	Reaction (4)[b]	Reaction (5)[c]	Reaction (6)[d] 25 mg L^{-1} FA	50 mg L^{-1} FA
0		*B. subtilis*	7.3 ± 0.1	11.6 ± 0.2	16.4 ± 0.1		
		S. oneidensis MR-1	7.6 ± 0.2	11.2 ± 0.1	15.6 ± 0.1		
		G. sulfurreducens	7.8 ± 0.2	11.6 ± 0.1	16.5 ± 0.1		
25, 50	4	*B. subtilis*				13.4 ± 0.2	13.4 ± 0.1
		S. oneidensis MR-1				13.8 ± 0.2	13.6 ± 0.3
		G. sulfurreducens				13.8 ± 0.1	13.6 ± 0.1
	6	*B. subtilis*				14.3 ± 0.1	14.0 ± 0.1
		S. oneidensis MR-1				14.4 ± 0.2	14.2 ± 0.3
		G. sulfurreducens				14.4 ± 0.2	14.2 ± 0.1
	8	*B. subtilis*				14.9 ± 0.2	14.4 ± 0.2
		S. oneidensis MR-1				14.9 ± 0.2	15.0 ± 0.4
		G. sulfurreducens				14.6 ± 0.3	14.6 ± 0.2
		Average value:				14.3 ± 0.2	14.1 ± 0.2

466 [a] $R\text{-}A_1^- + Hg^{2+} \Leftrightarrow R\text{-}A_1\text{-}Hg^+$

467 [b] $R\text{-}A_2^- + Hg^{2+} \Leftrightarrow R\text{-}A_2\text{-}Hg^+$

468 [c] $R\text{-}A_3^- + Hg^{2+} \Leftrightarrow R\text{-}A_3\text{-}Hg^+$

469 [d] $FA^- + Hg^{2+} \Leftrightarrow FA\text{-}Hg^+$. Both columns present the calculated log stability constant values for the adsorption of Hg to deprotonated FA, as expressed

470 in Reaction (6). The left column presents the values calculated from the 25 mg L^{-1} FA data, and the right column presents the values calculated from

471 the 50 mg L^{-1} FA data.

Figures


474
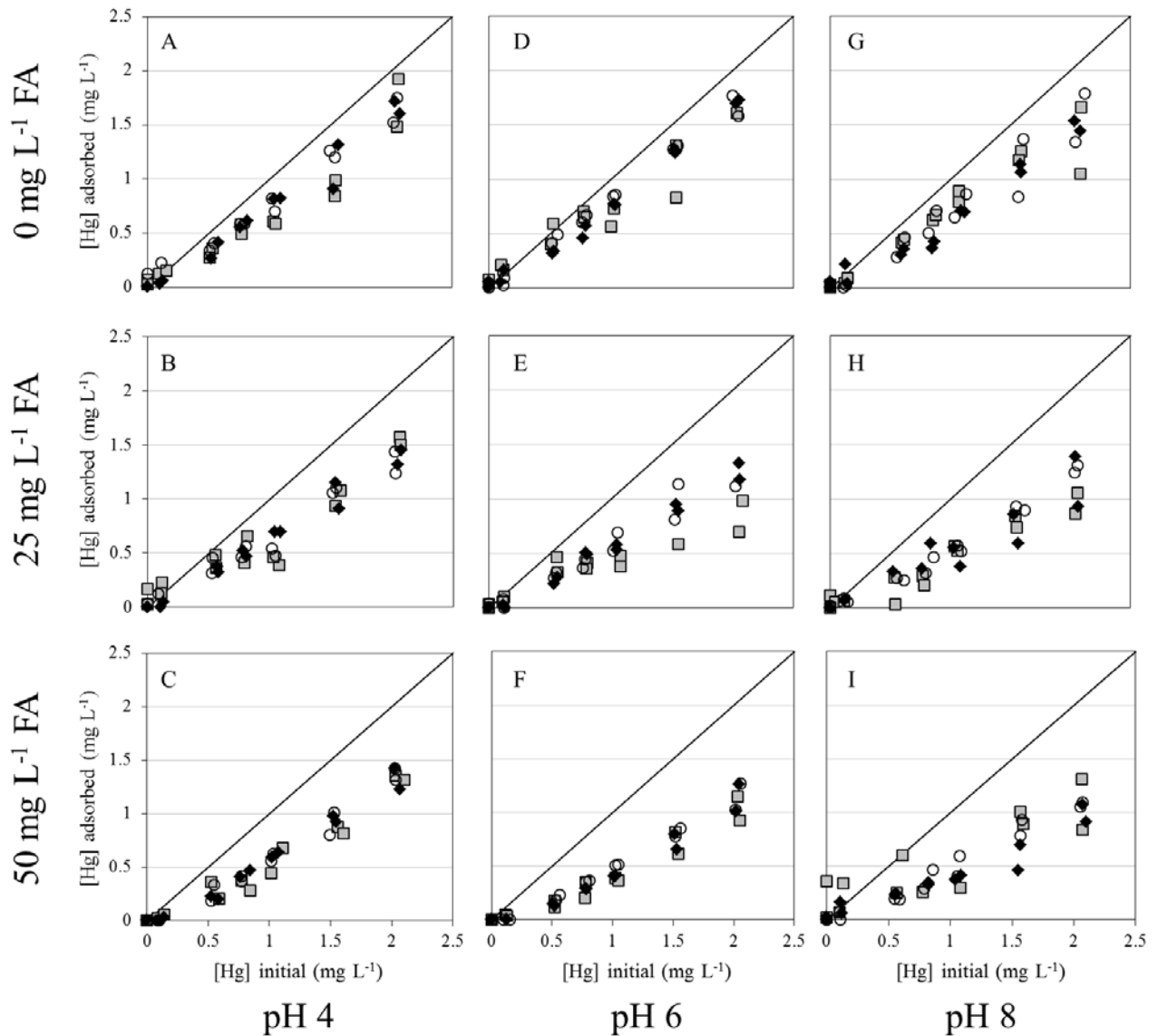
Figure 1: Aqueous chemistry results for Hg isotherms in the absence and presence of FA at pH 4

(A, B, C), pH 6 (D, E, F), and pH 8 (G, H, I). Plots A, D, and G present the results for the FA-

free controls, plots B, E, and H present the results for the 25 mg L^{-1} FA experiments, and plots C,

F, and I present the results of the 50 mg L^{-1} FA experiments. *B. subtilis* is represented by the

black-outlined, grey-filled squares, *S. oneidensis* MR-1 is represented by the solid black

480   diamonds, and *G. sulfurreducens* is represented by the hollow circles. The black line on each plot

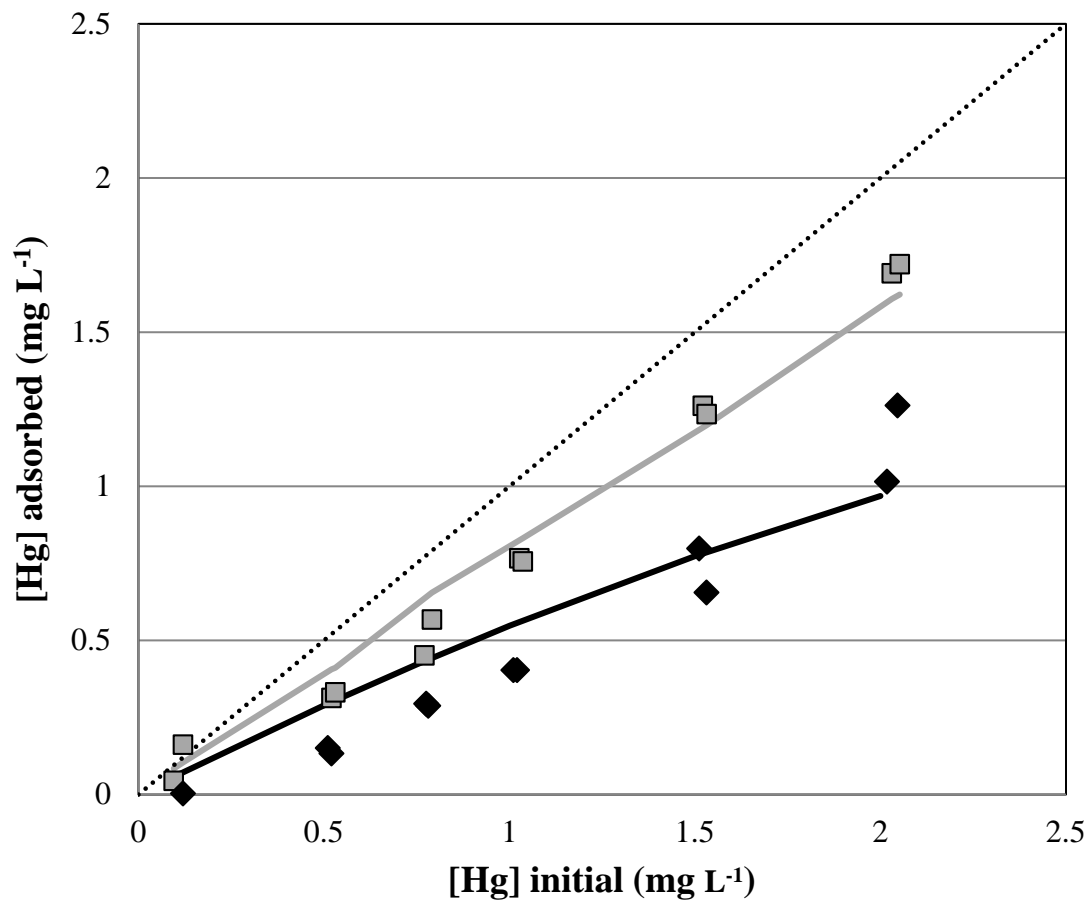481   represents 100% Hg adsorption under each experimental condition.

482
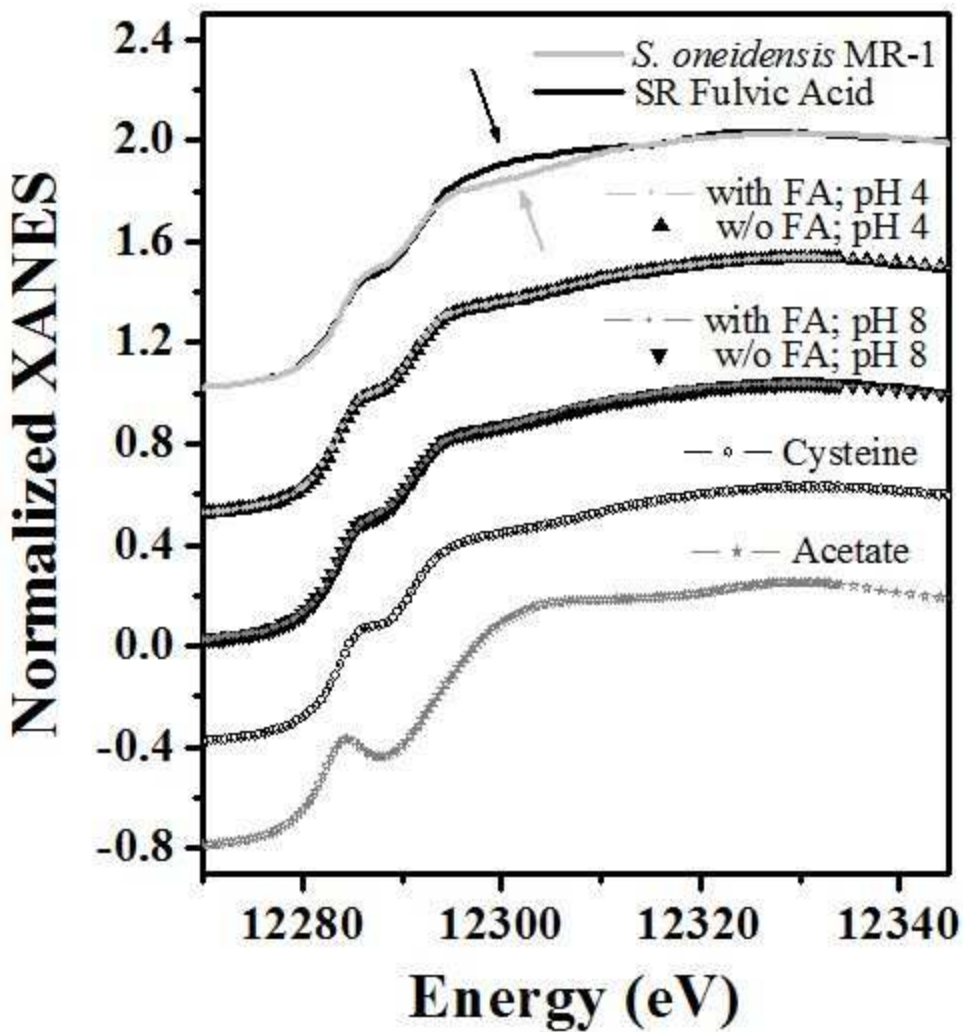
Figure 2: Hg L$_{III}$ edge XANES spectra of Hg bound to (from top to bottom) *S. oneidensis* MR-1
only at pH 4, FA only at pH 4, *S. oneidensis* MR-1 in the presence of 50 and 0 mg L^{-1} FA at pH
4, *S. oneidensis* MR-1 in the presence of 50 and 0 mg L^{-1} FA at pH 8, cysteine only, and acetate
only.

487
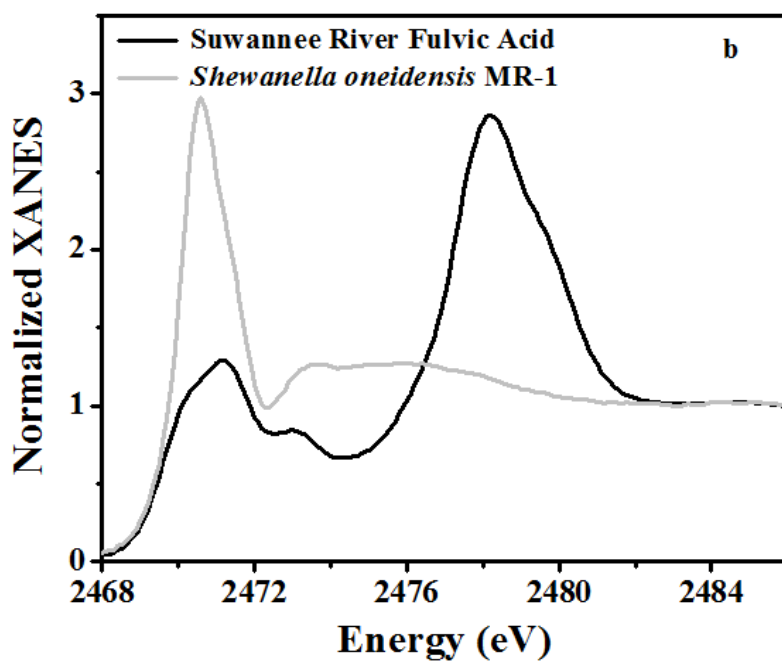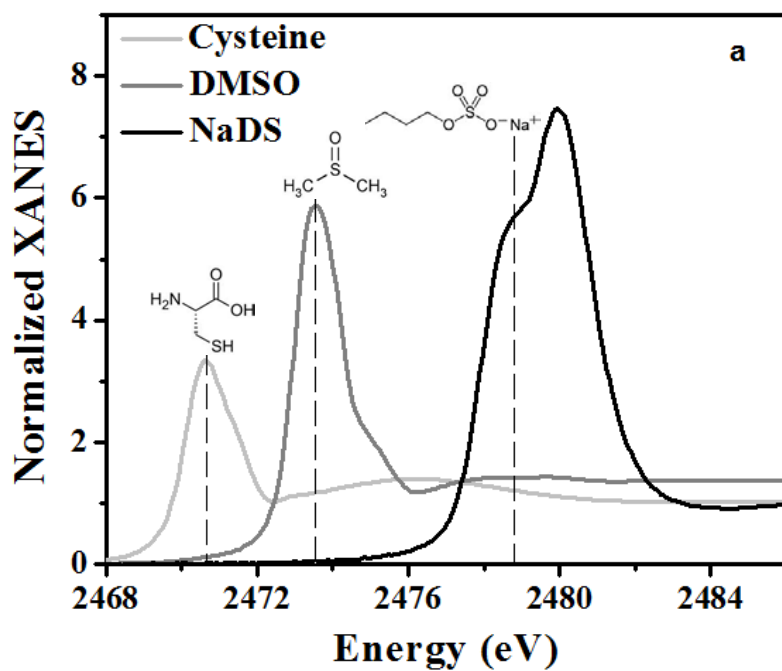
488

489   Figure 3: Sulfur K edge XANES spectra for a) cysteine, dimethyl sulfoxide (DMSO), and sodium

490   dodecyl sulfate (NaDS), and b) *S. oneidensis* MR-1 biomass and Suwannee River FA.

491

Figure 4: Representative model fits for *S. oneidensis* MR-1 at pH 6 under 0 mg L^{-1} FA (grey

squares and grey curve) and 50 mg L^{-1} FA (solid black diamonds and black curve) conditions.

The dotted line represents 100% Hg adsorption under each experimental condition.

495

Supplemental Information

497   Table S1: Hg reactions used in the speciation modeling.

Reaction	Log K
$H_2O - H^+ = OH^-$	-14.00 [b]
$H_2CO_3^0 - H^+ = HCO_3^-$	-6.355 [a]
$H_2CO_3^0 - 2H^+ = CO_3^{2-}$	-16.67 [a]
$H_2CO_3^0 - H_2O = CO_2^0$	2.770 [b]
$Na^+ + H_2CO_3^0 - 2H^+ = NaCO_3^-$	-15.41 [b]
$Na^+ + H_2CO_3^0 - H^+ = NaHCO_3^0$	-6.60 [b]
$Na^+ + H_2O - H^+ = NaOH^0$	-14.2 [b]
$Hg^{2+} + H_2O - H^+ = HgOH^+$	-3.40 [a]
$Hg^{2+} + 2H_2O - 2H^+ = Hg(OH)_2^0$	-5.98 [a]
$Hg^{2+} + 3H_2O - 3H^+ = Hg(OH)_3^-$	-21.1 [a]
$2Hg^{2+} + H_2O - H^+ = Hg_2(OH)^{3+}$	-3.30 [b]
$3Hg^{2+} + 3H_2O - 3H^+ = Hg_3(OH)_3^{3+}$	-6.40 [b]
$Hg^{2+} + H_2CO_3^0 - 2H^+ = HgCO_3^0$	-3.91 [a]
$Hg^{2+} + H_2CO_3^0 - H^+ = HgHCO_3^+$	0.42 [a]
$Hg^{2+} + H_2CO_3^0 + H_2O - 3H^+ = Hg(OH)CO_3^-$	-11.355 [a]
$B_1^- + H^+ = B_1\text{-}H^0$	
Bacillus subtilis	3.30 [c]
Shewanella oneidensis	3.30 [d]
Geobacter sulfurreducens	3.36 [e]
$B_2^- + H^+ = B_2\text{-}H^0$	
Bacillus subtilis	4.80 [c]
Shewanella oneidensis	4.80 [d]
Geobacter sulfurreducens	4.81 [e]
$B_3^- + H^+ = B_3\text{-}H^0$	
Bacillus subtilis	6.80 [c]
Shewanella oneidensis	6.70 [d]
Geobacter sulfurreducens	6.49 [e]
$FA^- + H^+ = FA\text{-}H^0$	5.85 [f]

498   [a] Powell et al., 2005.
499   [b] Martell and Smith, 2001.
500   [c] Fein et al., 2005
501   [d] Mishra et al., 2010
502   [e] Dunham-Cheatham et al.
503   [f] Calculated as the average of all reported pK_a values in Table 2 from Borrok and Fein (2004).
504   Assumed total site concentration is the sum of the average site concentrations for the individual
505   FA sites: 5.50×10^{-3} moles of sites per gram of humic substance.
506

507   Table S2: Best-fit values of Hg solution standards and Hg-biomass samples.

Sample	path	N	R(Å)	σ^2 (10^{-3} Å^2)
HgAc	Hg-O	1.78 ± 0.32	2.06 ± 0.01	10.9 ± 0.9
	Hg-C	1.78[a]	2.83 ± 0.01	12.8 ± 4.0
Hg-cysteine	Hg-S	1.88 ± 0.21	2.32 ± 0.01	10.5 ± 1.2
Hg-biomass (at pH 4)	Hg-S	1.85 ± 0.19	2.35 ± 0.01	10.2 ± 1.5
Hg-biomass (at pH 8)	Hg-S	1.70 ± 0.15	2.35 ± 0.01	11.0 ± 1.3

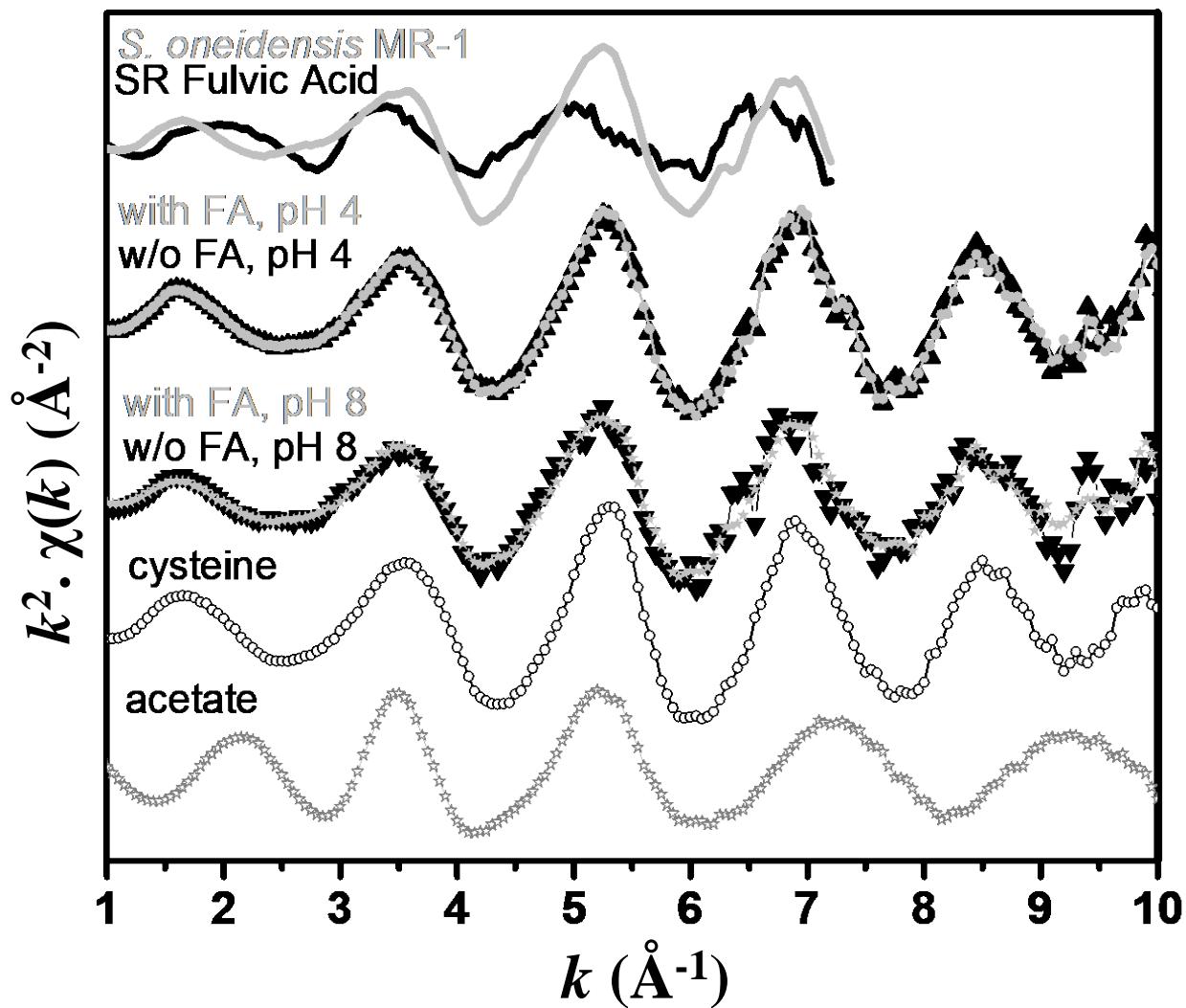508   [a] Set to Coordination number of O for this sample.

509

510

Sample	path	CN	R(Å)	σ^2 (10^{-3} Å^2)	Eo	χ_v^2	R
HgAc	Hg-O	1.78 ± 0.32	2.06 ± 0.01	10.9 ± 0.9	1.2 ± 0.9	48	0.63
	Hg-C	1.78[a]	2.83 ± 0.01	12.8 ± 4.0			
Hg-cysteine	Hg-S	1.88 ± 0.21	2.32 ± 0.01	10.5 ± 1.2	2.8 ± 0.6	22	0.45
Hg-biomass (at pH 4)	Hg-S	1.85 ± 0.19	2.35 ± 0.01	10.2 ± 1.5	3.0 ± 0.5	30	0.55
Hg-biomass (at pH 8)	Hg-S	1.70 ± 0.15	2.35 ± 0.01	11.0 ± 1.3			

511   [a] Set to Coordination number of O for this sample.

512

S. oneidensis MR-1
SR Fulvic Acid

with FA, pH 4
w/o FA, pH 4

with FA, pH 8
w/o FA, pH 8

cysteine

acetate

513

Figure S1: $k^2\gamma(k)$ EXAFS data for Hg L$_{III}$ edge EXAFS spectra of Hg bound to (top to bottom):
S. oneidensis MR-1 only at pH 4, FA only at pH 4, *S. oneidensis* MR-1 in the presence of 50 and
0 mg L^{-1} FA at pH 4, *S. oneidensis* MR-1 in the presence of 50 and 0 mg L^{-1} FA at pH 8, cysteine
only, and acetate only.
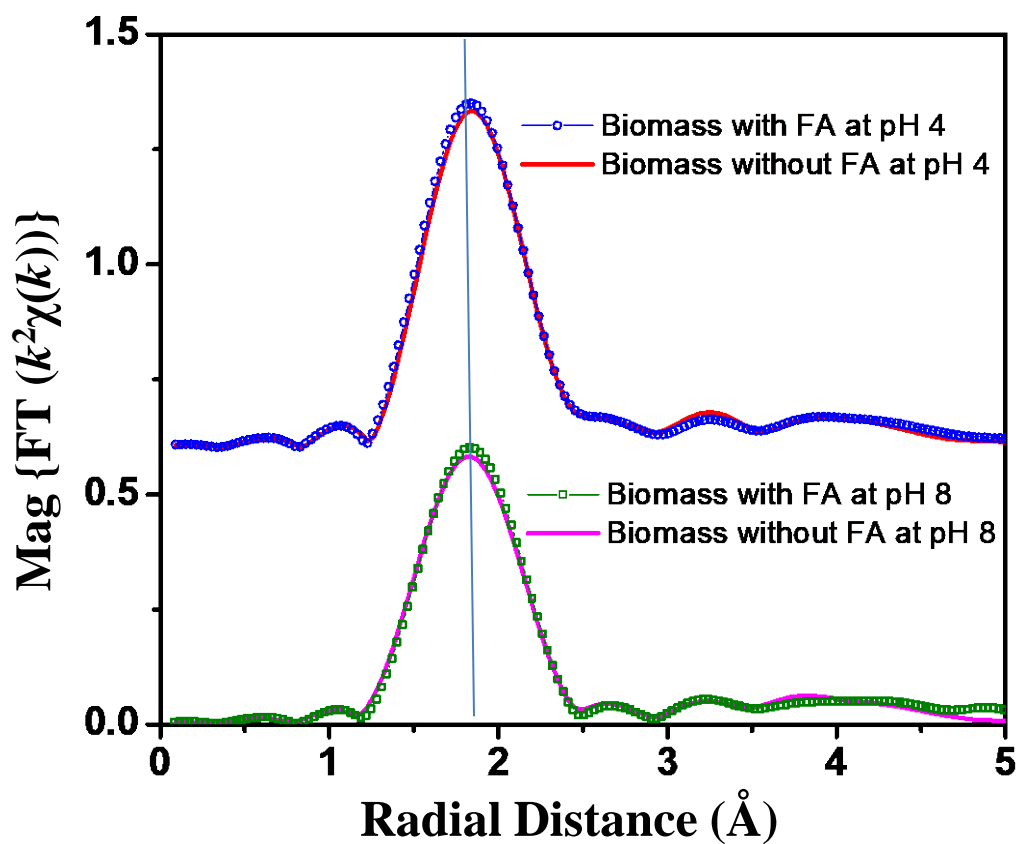
518

519 Figure S2: Magnitude of Hg L$_{III}$ edge EXAFS Fourier Transform (FT) data for Hg binding to *S.*

520 *oneidensis* MR-1 in the presence of 0 and 50 mg L^{-1} FA at pH 4 (top), and 0 and 50 mg L^{-1} FA at

521 pH 8 (bottom).

522

References

523

524 Benoit J. M., Gilmour C. C., Mason R. P., and Heyes A. (1999) Sulfide Controls on Mercury
525   Speciation and Bioavailability to Methylating Bacteria in Sediment Pore Waters. 33. 951-957.

526 Beveridge T. J., and Murray R. G. E. (1976) Uptake and retention of metals by cell walls of
527   Bacillus subtilis. Journal of Bacteriology. 127. 1502-1518.

528 Borrok D and Fein J. B. (2004) Distribution of protons and Cd between bacterial surfaces and
529   dissolved humic substances determined through chemical equilibrium modeling. Geochimica
530   et Cosmochimica Acta. 68. 3043-3052.

531 Borrok D., Turner B. F., and Fein J. B. (2005) A universal surface complexation framework for
532   modeling proton binding onto bacterial surfaces in geologic settings. American Journal of
533   Science. 305. 826-853.

534 Borrok D., Aumend K. and Fein J. B. (2007) Significance of ternary bacteria-metal-natural organic
535   matter complexes determined through experimentation and chemical equilibrium modeling.
536   Chemical Geology. 238. 44-62.

537 Colombo M. J., Ha J., Reinfelder J. R., Barkay T., Yee N. (2013) Anaerobic oxidation of Hg(0)
538   and methylmercury formation by *Desulfovibrio desulfuricans* ND132. Geochimica et
539   Cosmochimica Acta. 112. 166-177.

540 Compeau G. C., and Bartha R. (1987) Effect of salinity on mercury-methylating activity of sulfate-
541   reducing bacteria in estuarine sediments. Applied and Environmental Microbiology. 53. 261-
542   265.

543 Cox J. S., Smith D. S., Warren L. A., and Ferris F. G. (1999) Characterizing heterogeneous
544   bacterial surface functional groups using discrete affinity spectra for proton binding.
545   Environmental Science & Technology. 33. 4514-4521.

546 Croué J.-P., Benedetti D., Violleau D., and Leenheer J. A. (2003) Characterization and Copper
547   Binding of Humic and Nonhumic Organic Matter Isolated from the South Platte River:
548   Evidence for the Presence of Nitrogenous Binding Sites. Environmental Science &
549   Technology. 37. 328-336.

550 Daughney C. J., Siciliano S. D., Rencz A. N., Lean D., and Fortin D. (2002) Hg(II) adsorption by
551   bacteria: A surface complexation model and its application to shallow acidic lakes and
552   wetlands in Kejimkujik National Park, Nova Scotia, Canada. Environmental Science &
553   Technology. 36. 1546-1553.

554 Dong W. M., Bian Y. R., Liang L. Y., and Gu B. H. (2011) Binding Constants of Mercury and
555   Dissolved Organic Matter Determined by a Modified Ion Exchange Technique. Environmental
556   Science & Technology. 45. 3576-3583.

557 Drexel R. T., Haitzer M., Ryan J. N., Aiken G. R., and Nagy K. L. (2002) Mercury(II) Sorption to
558   Two Florida Everglades Peats: Evidence for Strong and Weak Binding and Competition by
559   Dissolved Organic Matter Released from the Peat. Environmental Science & Technology. 36.
560   4058-4064.

561 Dunham-Cheatham S., Farrell B., Mishra B., Myneni S., and Fein J. B. The effect of chloride on
562   the adsorption of Hg onto three bacterial species. Manuscript submitted for publication.

563 Ephraim J. H. (1992) Heterogeneity as a concept in the interpretation of metal ion binding by
564   humic substances. The binding of zinc by an aquatic fulvic acid. Analytica Chimica Acta. 267.
565   39-45.

566 Fein J. B., Boily J.-F., Yee N., Gorman-Lewis D., and Turner B. F. (2005) Potentiometric titrations
567   of Bacillus subtilis cells to low pH and a comparison of modeling approaches. Geochimica et
568   Cosmochimica Acta. 69. 1123-1132.

569 Fein, J.B., 2006. Thermodynamic modeling of metal adsorption onto bacterial cell walls: current
570   challenges. Adv. Agron. 90, 179–202.

571 Fortin D. and Beveridge T. J. (1997) Role of the bacterium Thiobacillus in the formation of
572   silicates in acidic mine tailings. Chemical Geology. 141. 235-250.

573 Guiné V., Spadini L., Sarret G., Muris M., Delolme C., Gaudet J. P., and Martins J. M. F. (2006)
574   Zinc sorption to three gram-negative bacteria: Combined titration, modeling, and EXAFS
575   study. Environmental Science & Technology. 40. 1806-1813.

576 Haitzer M., Aiken G. R., and Ryan J. N. (2002) Binding of Mercury(II) to Dissolved Organic
577   Matter: The Role of the Mercury-to-DOM Concentration Ratio. Environmental Science &
578   Technology. 36. 3564-3570.

579 Haitzer M., Aiken G. R., and Ryan J. N. (2003) Binding of Mercury(II) to Aquatic Humic
580   Substances: Influence of pH and Source of Humic Substances. Environmental Science &
581   Technology. 37. 2436-2441.

582 Harris, H. H., Pickering, I. J., George, G. N. (2003) The Chemical Form of Mercury in
583   Fish.Science. 301. 1203.

584 Hesterberg D., Chou J. W., Hutchison K. J., and Sayers D. E. (2001) Bonding of Hg(II) to Reduced
585   Organic Sulfur in Humic Acid as Affected by S/Hg Ratio. Environmental Science &
586   Technology. 35. 2741-2745.

587 Johnson K. J., Szymanowski J. E. S., Borrok D., Huynh T. Q., and Fein J. B. (2007) Proton and
588   metal adsorption onto bacterial consortia: Stability constants for metal-bacterial surface
589   complexes. Chemical Geology. 239. 13-26.

590 Kenney J. P. L. and Fein J. B. (2011) Cell wall reactivity of acidophilic and alkaliphilic bacteria
591   determined by potentiometric titrations and Cd adsorption experiments. Environmental
592   Science & Technology. 45. 4446-4452.

593 Loux, N. T. (1998) An assessment of mercury-species-dependent binding with natural organic
594   carbon. Chemical Speciation and Bioavailability. 10. 127-136.

595 Lovely, D.R. and Phillips, E.J.P. (1988) Novel mode of microbial energy metabolism: organic
596   carbon oxidation coupled to dissimilatory reduction of iron or manganese. Applied and
597   Environmental Microbiology. 54. 1472-1480.

598 Martell A. E. and Smith R. M. (2001) NIST Critically selected stability constants of metal
599   complexes, Version 6.0. NIST Standard Reference Database. 46. National Institute of
600   Standards and Technology. Gaithersburg, MD.

601 McDowell W. H. (2003) Dissolved organic matter in soils – future directions and unanswered
602   questions. Geoderma. 113. 179-186.

603 Mishra, B., Fein, J. B., Boyanov, M. I., Kelly, S. D., Kemner, K. M., Bunker, B. A. (2007)
604   Comparison of Cd Binding Mechanisms by Gram-Positive, Gram-Negative and Consortia of
605   Bacteria Using XAFS. AIP Conference proceeding. 882. 343-345.

606 Mishra B., Boyanov M. I., Bunker B. A., Kelly S. D., Kemner K. M., Nerenberg R., Read-Daily
607   B.L., and Fein J. B. (2009) An X-ray absorption spectroscopy study of Cd binding onto
608   bacterial consortia. *Geochimica et Cosmochimica Acta.* 73. 4311-4325.

609 Mishra B., Boyanov M., Bunker B. A., Kelly S. D., Kemner K. M., and Fein J. B. (2010) High-
610   and low-affinity binding sites for Cd on the bacterial cell walls of Bacillus subtilis and
611   Shewanella oneidensis. *Geochimica et Cosmochimica Acta.* 74. 4219-4233.

612 Mishra, B., O'Loughlin, E. J., Boyanov. M.B.,, Kemner, K. M. (2011) Binding of HgII to High-
613   Affinity Sites on Bacteria Inhibits Reduction to Hg^0 by Mixed $Fe^{II/III}$ Phases. Environmental
614   Science & Technology. 45. 9597-9603.

615 Morra, M.J., Fendorf, S. E., Brown, P. D. (1997) Speciation of sulfur in humic and fulvic acids
616   using X-ray absorption near-edge structure (XANES) spectroscopy. Geochimica et
617   Cosmochimica Acta. 61. 683-688.

618 Muresan B., Pernet-Coudrier B., Cossa D., and Varrault G. (2011) Measurement and modeling of
619   mercury complexation by dissolved organic matter isolates from freshwater and effluents of a
620   major wastewater treatment plant. Applied Geochemistry. 26. 2057-2063.

621 Myneni, S. C. B. (2002) Soft X-ray spectroscopy and spectromicroscopy studies of organic
622   molecules in the environment. Reviews in Mineralogy and Geochemistry. 49. 485-579.

623 Pokrovsky O.S., Pokrovski G. S., Shirokova L.S., Gonzalez A. G., Emnova E. E., Feurtet-Mazel
624   A. (2012) Chemical and structural status of copper associated with oxygenic and anoxygenic
625   phototrophs and heterotrophs: possible evolutionary consequences. Geobiology. 10. 130-149.

626 Powell K. J., Brown P. L., Byrne R. H., Gajda T., Hefter G., Sjoberg S., and Wanner H. (2005)
627   Chemical speciation of environmentally significant heavy metals with inorganic ligands. Part
628   1: The Hg^{2+}-Cl^-, OH^-, CO_3^{2-}, SO_4^{2-}, and PO_4^{3-} aqueous systems. Pure and Applied Chemistry.
629   77. 739-800.

630 Ravel, B., Newville,M. (2005) ATHENA, ARTEMIS, HEPHAESTUS: Data analysis for X-ray
631   absorption spectroscopy using IFEFFIT. Journal of Synchrotron Radiation. 12. 537–541.

632 Ravichandran M., Aiken G. R., Ryan J. N., and Reddy M. M. (1999) Inhibition of precipitation
633   and aggregation of metacinnabar (mercuric sulfide) by dissolved organic matter isolated from
634   the Florida Everglades. Environmental Science & Technology. 33. 1418-1423.

635 Ravichandran M. (2004) Interactions between mercury and dissolved organic matter – a review.
636   Chemosphere. 55. 319-331.

637 Skyllberg U., Bloom P. R., Qian J., Lin C.-M., and Bleam W. F. (2006) Complexation of
638   Mercury(II) in Soil Organic Matter: EXAFS Evidence for Linear Two-Coordination with
639   Reduced Sulfur Groups. Environmental Science & Technology. 40. 4174-4180.

640 Segre, C. U., Leyarovsky, N. E., Chapman, L. D., Lavender, W. M., Plag, P. W., King, A. S.,
641   Kropf, A. J., Bunker, B. A., Kemner, K. M., Dutta, P., Duran, R. S., Kaduk, J. (2000) The
642   MRCAT insertion device beamline at the Advanced Photon Source, CP521. Synchrotron

Radiation Instrumentation: Eleventh U.S. National Conference; Pianetta, P., Ed.; American Institute of Physics:NewYork, 419–422.

Song Z., Kenney J. P. L., Fein J. B., Bunker B. A. (2012) An X-Ray Absorption Fine Structure study of Au adsorbed onto the non-metabolizing cells of two soil bacterial species. Geochimica et Cosmochimica Acta. 86. 103-117.

Stern, E. A., Newville, M., Ravel, B., Yacoby, Y., Haskel, D. (1995) The UWXAFS analysis package philosophy and details. Physica B. 209. 117–120.

Vairavamurthy, A. (1998) Using X-ray absorption to probe sulfur oxidation states in complex molecules. Spectrochimica Acta Part A: Molecular and Biomolecular Spectroscopy. 54. 2009-2017.

Westall J. C. (1982) FITEQL, A computer program for determination of chemical equilibrium constants from experimental data. Version 2.0. Report 82-02, Department of Chemistry, Oregon State University, Corvallis, OR, USA.

Wightman P. G. and Fein J. B. (2001) Ternary interactions in a humic acid-Cd-bacteria system. Chemical Geology. 180. 55-65.

Winfrey M. R. and Rudd J. W. M. (1990) Environmental factors affecting the formation of methylmercury in low pH lakes. Environmental Toxicology and Chemistry. 9. 853-869.

Xia K., Skyllberg U. L., Bleam W. F., Bloom P. R., Nater E. A., and Helmke P. A. (1999) X-ray Absorption Spectroscopic Evidence for the Complexation of Hg(II) by Reduced Sulfur in Soil Humic Substances. Environmental Science & Technology. 33. 257-261.

Xia K., Weesner, F., Bleam W.F., Helmke P.A., Bloom P.R., Skyllberg U.L. (1998) XANES Studies of Oxidation States of Sulfur in Aquatic and Soil Humic Substances. Soil Science Society of America Journal. 62. 124-1246.

Yee N. and Fein J. B. (2001) Cd adsorption onto bacterial surfaces: A universal adsorption edge? Geochimica et Cosmochimica Acta. 65. 2037.